TISSUE ENGINEERING: Part A
Volume 19, Numbers 7 and 8, 2013

DOI: 10.1089/ten.tea.2012.0172

Human Embryonic Stem Cell-Derived Mesenchymal Stem Cell Seeding on Calcium Phosphate Cement-Chitosan-RGD Scaffold for Bone Repair

Wenchuan Chen, DDS, PhD,[1,2] Hongzhi Zhou, DDS, PhD,[1,3] Michael D. Weir, PhD,[1] Minghui Tang, PhD,[1] Chongyun Bao, DDS, PhD,[2] and Hockin H.K. Xu, PhD[1,4–6]

Calcium phosphate cement (CPC) has *in situ*-setting ability and excellent osteoconductivity. Human embryonic stem cells (hESCs) are exciting for regenerative medicine due to their strong proliferative ability and multilineage differentiation capability. However, there has been no report on hESC seeding with CPC. The objectives of this study were to obtain hESC-derived mesenchymal stem cells (hESCd-MSCs), and to investigate hESCd-MSC proliferation and osteogenic differentiation on novel CPC with chitosan immobilized with RGD (CPC-chitosan-RGD). RGD was covalently bonded with chitosan, which was then incorporated into CPC. The CPC-chitosan-RGD scaffold had higher strength and toughness than CPC-chitosan control without RGD ($p < 0.05$). hESCs were cultured to form embryoid bodies (EBs), and the MSCs were then migrated out of the EBs. Flow cytometry indicated that the hESCd-MSCs expressed typical surface antigen profile of MSCs. hESCd-MSCs had good viability when seeded on CPC scaffolds. The percentage of live cells and the cell density were significantly higher on CPC-chitosan-RGD than CPC-chitosan control. Scanning electron microscope examination showed hESCd-MSCs with a healthy spreading morphology adherent to CPC. hESCd-MSCs expressed high levels of osteogenic markers, including alkaline phosphatase, osteocalcin, collagen I, and Runx2. The mineral synthesis by the hESCd-MSCs on the CPC-chitosan-RGD scaffold was twice that for CPC-chitosan control. In conclusion, hESCs were successfully seeded on CPC scaffolds for bone tissue engineering. The hESCd-MSCs had good viability and osteogenic differentiation on the novel CPC-chitosan-RGD scaffold. RGD incorporation improved the strength and toughness of CPC, and greatly enhanced the hESCd-MSC attachment, proliferation, and bone mineral synthesis. Therefore, the hESCd-MSC-seeded CPC-chitosan-RGD construct is promising to improve bone regeneration in orthopedic and craniofacial applications.

Introduction

Bone defects often arise from infections, trauma, tumor resections, abnormal development, and congenital malformations, which require more than 500,000 bone grafts annually in the United States.[1] Regenerative medicine offers an exciting approach for bone repair and regeneration, which involves the synergistic combination of stem cells with suitable scaffolds.[2–4] Stem cells have the ability to differentiate into one or more tissue types. Studies have shown exciting results on stem cell delivery via scaffolds for tissue regeneration.[5–7] Currently, human embryonic stem cells (hESCs) and adult stem cells are the two major cell sources in regenerative medicine.[8–16]

Adult stem cells have been isolated from a wide variety of tissues. Many tissues contain putative adult stem cell populations with osteogenic potential, including bone marrow, periosteum, synovium, trabecular bone, fat, muscle, lung, and deciduous teeth. Of particular interest are human bone marrow mesenchymal stem cells (hBMSCs) or osteoprogenitor cells, which are considered to be the principal source of cells for bone engineering. hBMSCs possess several advantages, such as availability from an autologous source, relatively high proliferative capacity, and multilineage differentiation potential. However, the use of hBMSCs has limitations. First, the self-renewal and proliferative ability of hBMSCs decreases due to aging [17–19] and diseases, such as osteoporosis and arthritis.[20,21] Second, the heterogeneity of

[1]Biomaterials & Tissue Engineering Division, Department of Endodontics, Prosthodontics and Operative Dentistry, University of Maryland Dental School, Baltimore, Maryland.
[2]State Key Laboratory of Oral Diseases, West China College of Stomatology, Sichuan University, Chengdu, China.
[3]Department of Oral & Maxillofacial Surgery, School of Stomatology, Fourth Military Medical University, Xi'an, China.
[4]Center for Stem Cell Biology and Regenerative Medicine, University of Maryland School of Medicine, Baltimore, Maryland.
[5]Marlene and Stewart Greenebaum Cancer Center, University of Maryland School of Medicine, Baltimore, Maryland.
[6]Department of Mechanical Engineering, University of Maryland, Baltimore County, Maryland.

adult stem cells from bone marrow indicates that only a very small proportion of cells can be considered stem cells and can differentiate into the osteogenic lineage.[22] In this regard, hESCs hold great promise. hESCs are relatively homogenous, possess a high self-renewal activity, have no limits in proliferation, and can be differentiated into any cell type except those needed to develop the placenta. Recently, several studies investigated the use of hESCs for bone tissue engineering, and demonstrated that hESCs could undergo osteogenic differentiate *in vitro* and *in vivo*.[13,23–25]

Besides cells, scaffolds are another important component for tissue engineering.[26] Bioceramics, such as calcium phosphates are important for bone repair, because they can bond to bone to form a functional interface due to their compositions mimicking bone minerals to enhance cell attachment.[27–30] They are also a good system to delivery drug or growth factor for bone tissue engineering.[31,32] However, for a prefabricated bioceramic to fit into a bone cavity, the surgeon needs to machine the graft or carve the surgical site, leading to increases in bone loss, trauma, and surgical time.[3] On the other hand, injectable scaffolds can be used in minimally invasive procedures and fit intimately into bone defects.[3,33,34] Calcium phosphate cements (CPCs) are injectable and have good bioactivity and osteoconductivity. The first CPC comprised of tetracalcium phosphate [TTCP: $Ca_4(PO_4)_2O$] and dicalcium phosphate anhydrous (DCPA: $CaHPO_4$), and was termed CPC.[35] The CPC powder can be mixed with an aqueous liquid to form a paste that can be injected or sculpted during surgery to conform to the defect in hard tissues.[36,37] CPC was approved in 1996 by the Food and Drug Administration for repairing craniofacial defects, thus becoming the first CPC for clinical use.[38] Traditional CPC was brittle and weak; however, the mechanical properties of CPC were improved by incorporating chitosan.[39,40] The CPC-chitosan scaffold supported the adhesion and proliferation of osteoblast cells and hMSCs.[39,40] However, to date, there has been no report on hESC-derived MSC seeding on CPC.

The objectives of this study were to investigate hESC-derived MSC seeding on the CPC-chitosan scaffold immobilized with RGD, and to examine the effect of RGD in CPC on the proliferation and osteogenic differentiation of hESC-derived MSCs for the first time. Cell attachment on biomaterials is an important regulator of many cellular functions, such as proliferation and differentiation. However, previous studies showed that human stem cell attachment to CPC was relatively poor.[40,41] Therefore, there is a need to improve the cell attachment to CPC. Two hypotheses were tested: (1) hESC-derived MSCs can successfully undergo osteogenic differentiation on the CPC-chitosan scaffold; (2) RGD incorporation will greatly enhance hESC-derived MSC attachment, osteogenic differentiation, and synthesis of bone minerals on the CPC-chitosan scaffold.

Materials and Methods

Fabrication of CPC and CPC-RGD specimens

The CPC powder consisted of an equimolar mixture of DCPA and TTCP. Chitosan has been shown to strengthen CPC,[39] resist the washout of CPC paste in a physiological solution, and cause fast-setting to CPC.[42] Hence, the CPC liquid consisted of chitosan mixed with distilled water at a chitosan/(chitosan + water) mass fraction of 15%.[42] The previous studies did not report RGD incorporation into CPC.[39,42] In the present study, two types of chitosan were used: chitosan malate (Halosource, Redmond, WA) and RGD-modified chitosan malate.

The protocol for immobilizing RGD in chitosan was similar to that reported in a previous study.[43] RGD-immobilized chitosan was synthesized by coupling G4RGDSP (Thermo Fisher, Waltham, MA) with chitosan. The amide bond was formed between carboxyl groups in peptide and residual amine groups in chitosan using 1-ethyl-3-[3-dimethylaminopropyl] carbodiimide hydrochloride (EDC) and sulfo-*N*-hydroxysuccinimide (Sulfo-NHS; Thermo Fisher) as coupling agents. After dissolving the G4RGDSP peptide (12.4 mg, 16.32×10^{-6} mol) in a 0.1 M 2-(N-Morpholino) ethanesulfonic acid (MES) buffer (4 mL; Thermo Fisher), EDC (3.76 mg, 19.6×10^{-6} mol) and Sulfo-NHS (0.28 mg, 2.44×10^{-6} mol) were added to the peptide solution (molar ratio of G4RGDSP:EDC:NHS = 1:1.2:0.6). The solution was incubated at room temperature for 30 min to activate the terminal carboxyl group of serine. Then, this solution was added to the chitosan solution dissolved in the 0.1 M MES buffer (100 mL, 1 wt%). The coupling reaction was performed for 24 h at room temperature. The product was dialyzed against distilled water using a Dialysis Cassettes (MWCO = 3.5 kDa) (Thermo Fisher) for 3 days to remove uncoupled peptides by changing water three times daily. This process yielded RGD-modified chitosan, which was freeze-dried.

The CPC powder was mixed with chitosan liquid at a powder to liquid mass ratio of 2 to 1 to form a flowable paste. The paste was placed in 3-×4-×25-mm molds to fabricate bars for mechanical testing, and disk molds of 12 mm in diameter and 2 mm in thickness to make CPC disks for cell study. Two groups were tested: CPC using the chitosan without RGD is referred to as CPC-chitosan control, and CPC using RGD-modified chitosan is referred as CPC-chitosan-RGD.

CPC setting time and mechanical property measurement

To measure the setting time of CPC-chitosan control and CPC-chitosan-RGD, each paste was mixed and placed into a mold of $3\times4\times25$ mm. The assembly was kept in a humidor at 37°C. Following a previous study, the specimen was scrubbed gently with fingers.[42] This was done at 1-min intervals until the powder component did not come off from the specimen. This indicates that the setting reaction had occurred sufficiently to hold the specimen together.[42] The time from the CPC powder–liquid mixing to this point was measured as the setting time.

The specimen was incubated in a humidor at 100% humidity and 37°C for 4 h, then demolded, and immersed in distilled water for 20 h at 37°C.[42] Mechanical properties were tested in three-point flexure with 20-mm span at a crosshead speed of 1 mm/min on a computer-controlled Universal Testing Machine (MTS, Eden Prairie, MN).[39] Flexural strength was calculated as: $S = 3F_{max}L/(2bh^2)$, where F_{max} is the maximum load on the load–displacement (F-d) curve, L is span, b is specimen width, and h is specimen thickness. Elastic modulus was calculated as: $E = (F/d)(L^3/[4bh^3])$,

where F/d is the slope in the linear-elastic region. Work-of-fracture (toughness) was calculated as the area under the F-d curve divided by the specimen's cross-sectional area.[42]

Culture and propagation of hESCs

hESCs were obtained from Wicell (Madison, WI) and were of the H9 line listed on the National Institute of Health (NIH) registry. The use of hESCs was approved by the University of Maryland. hESCs were cultured according to the recommended protocol of Wicell.[44] Undifferentiated hESCs were cultured as colonies (example from this study shown in Fig. 2A) on a feeder layer of mitotically inactivated mouse embryonic fibroblasts (MEF), which was formed by seeding 200,000 MEF cells/well on Nunclon Δ Surface six-well culture plates (Nunc, Rochester, NY). Mitotic inactivation was achieved through exposure to 10 μg/mL Mitomycin C (Sigma, St. Louis, MO) for 2 h. The hESCs culture medium consisted of 80% (v/v) Dulbecco's modified Eagle's medium (DMEM)/F12 (Invitrogen, Carlsbad, CA), 20% Knockout Serum Replacement (a serum-free formulation; Invitrogen), 1 mM glutamine (Sigma), 0.1 mM 2-Mercaptoethanol (Sigma), 1% MEM nonessential amino acids solution (Invitrogen), and 4 ng/mL basic fibroblast growth factor (β-FGF; Invitrogen). Cells were cultured at 37°C with 5% CO_2 and 100% humidity, and the medium was changed daily. Colonies demonstrating differentiated morphologies were individually selected and mechanically removed with fire-thrown Pasteur pipettes to ensure the undifferentiated expansion of hESCs. Routine serial passage of hESCs was achieved through mild enzymatic dissociation of hESCs colonies with 1 mg/mL collagenase type IV (Gibco, Gaithersburg, MD) for 5 min, followed by seeding on a fresh inactivated MEF layer.

MSC derivation from hESCs

To simulate spontaneous differentiation, the hESCs were induced to form embryoid bodies (EBs).[23] Briefly, hESC colonies were dissociated into clumps through treatment with 1 mg/mL collagenase type IV for an extended duration of 10 min, followed by mechanical scraping. The dissociated hESC clumps were then transferred to 25-cm^2 ultra-low attachment cell culture flasks (Corning, Corning, NY) in a EB formation medium, which consisted of the DMEM (Gibco) supplemented with 20% fetal bovine serum defined (Gibco), 1 mM glutamine (Sigma), 0.1 mM 2-Mercaptoethanol (Sigma), and 1% MEM nonessential amino acids solution (Gibco). Initially, the hESC clumps were largely composed of densely packed hESCs, creating simple EBs. After 4–5 days of suspension culture in the presence of an ultra-low attachment surface, the center of the bodies became cavitated, and the bodies began to accumulate fluid and turn into free floating EBs (Fig. 2B). The culture medium was changed every 2 days. After 10 days, the EBs were transferred into Nunclon Δ Surface six-well culture plates and cultured for 10 additional days. After 2 days, most of the EBs adhered and many cells migrated out from the edges of the EBs. Upon 70% confluence, the outgrowth of cells were selectively isolated by using cell scrapers and subcultured at an initial cell density of 2×10^4 cells/cm^2 in the MSC growth medium, which consisted of the DMEM (Gibco) supplemented with 10% FBS (HyClone, Logan, UT), 2 mM L-glutamine (Gibco), 100 U/mL penicillin, and 100 mg/mL streptomycin (Gibco). Differentiated cells derived from these culture conditions were termed hESC-derived MSCs, or hESC-derived mesenchymal stem cells (hESCd-MSCs, Fig. 2C) and used in this study.

Flow cytometry of hESCd-MSCs

Expression of the cell surface antigen profile of hESCd-MSCs was characterized using flow cytometry.[23] hESCd-MSCs (passage 4) were harvested by trypsin-EDTA and washed with cold phosphate-buffered saline (PBS) containing 1% bovine serum albumin (BSA), then resuspended to approximately 1×10^6 cells in 50 μL of cold PBS containing 1% BSA. Cell samples were separately labeled on ice with optimal dilution of fluorescein isothiocyanate-conjugated monoclonal antibodies (mAbs; all from Invitrogen, except when indicated) against CD29, CD31, CD34 (BD, San Jose, CA), CD44, CD45, CD73 (BD), TRA-1-81 (BD), HLA-ABC, HLA-DR, phycoerythrin-conjugated mAbs against Oct3/4 (BD) and CD166 (BD), and Alexa Fluor 488-conjugated mAb against CD105 in the dark. After 30-min incubation, cells were washed with cold PBS containing 1% BSA. Nonspecific fluorescence was determined by incubating cells with isotype-matched-conjugated mAbs. At least 10,000 events were collected from each run of flow cytometry. Data were analyzed using CellQuest software (Becton Dickinson, San Jose, CA). The fluorescence histogram for each mAb was displayed alongside the control antibody. Percentages of positive cells were subtracted from the isotype control antibody of each conjugate.

Viability of hESCd-MSCs on CPC scaffolds

A cell suspension of 150,000 hESCd-MSCs at passage 4 in 2 mL of an osteogenic medium was added to each well of a 24-well plate containing a CPC disk. The osteogenic medium consisted of the MSC growth medium supplemented with 50 μM ascorbic acid-2-phosphate, 10 mM β-glycerophosphate, 100 nM dexamethasone, and 10 nM 1α,25-Dihydroxyvitamin (Sigma). The medium was changed daily. After 1, 4, 7, or 14 days, the medium was removed and the CPC disks were washed two times with 2 mL of PBS. The cells were live/dead stained and viewed by epifluorescence microscopy (TE2000-S; Nikon, Melville, NY). Staining was done for 30 min with 2 mL of PBS containing 2 μM calcein-AM and 2 μM ethidium homodimer-1 (Molecular Probes, Eugene, OR). Two parameters were measured following a previous study.[40] The first was the percentage of live cells, P_L, which was calculated as: $P_L = N_L/(N_L + N_D)$, where N_L = number of live cells, and N_D = number of dead cells, in the same image. Three randomly chosen fields of view were photographed for each specimen. Five specimens of each material ($n = 5$) yielded 15 photos for each time point. The second parameter was live cell density: $D_L = N_L/A$, where A is the area of the view field in which N_L was measured.

Quantitative real-time reverse transcription–polymerase chain reaction measurement of osteogenic differentiation of hESCd-MSCs on CPC

Osteogenic differentiation of hESCd-MSCs attaching to CPC was measured via quantitative real-time reverse

transcription–polymerase chain reaction (qRT-PCR; 7900HT, Applied Biosystems, Foster City, CA). At 1, 4, 7, and 14 days, the total cellular RNA on the scaffolds was extracted with the TRIzol reagent and the PureLink RNA Mini Kit (Invitrogen), and then reverse transcribed into cDNA using a High-Capacity cDNA Archive Kit in a Thermal Cycler (GenAmp PCR 2720; Applied Biosystems). TaqMan gene expression assay kits, including two predesigned specific primers and probes, were used to measure the transcript levels of the proposed genes on human alkaline phosphatase (ALP, Hs00758162_m1), osteocalcin (OC, Hs00609452_g1), collagen type I (Coll I, Hs00164004), Runx2 (Hs00231692_ml), and glyceraldehyde 3-phosphate dehydrogenase (GAPDH, Hs99999905). Relative expression level for each target gene was evaluated using the $2^{-\Delta\Delta Ct}$ method.[45] The C_t values of target genes were normalized by the C_t values of the human housekeeping gene, GAPDH, to obtain the ΔC_t values. The C_t value of hESCd-MSCs cultured on tissue culture polystyrene in the MSC growth medium for 1 day served as the calibrator.

Mineral synthesis by hESCd-MSCs

Mineral synthesis by hESCd-MSCs was investigated at 7, 14, and 21 days. These time periods were selected because previous studies showed that a great increase in the calcium content was observed during *in vitro* cell cultures between 12 to 21 days.[46] CPC disks with hESCd-MSCs cultured in the osteogenic medium were fixed with 10% formaldehyde and stained with Alizarin Red S (ARS; Millipore, Billerica, MA), which stained calcium-rich deposits by cells into a red color. An osteogenesis assay (Millipore) was used to extract the stained minerals and measure the ARS concentration, following the manufacturer's instructions. Control scaffolds with the same compositions, but without cells, were measured at the same time periods; they were subjected to the same culture medium and incubation conditions as the cell-seeded disks. The control's ARS concentration was subtracted from that of the corresponding scaffold with cells to yield the net mineral concentration synthesized by the cells.

Scanning electron microscopy and statistical analysis

A scanning electron microscope (SEM; JEOL 5300, Peabody, MA) was used to examine the hESCd-MSC attachment on CPC. Specimens with cells cultured for 4 days were rinsed with PBS, fixed with 1% glutaraldehyde, subjected to graded alcohol dehydrations, rinsed with hexamethyldisilazane, sputter-coated with gold, and examined in SEM. In addition, the cross sections of fractured CPC specimens from mechanical testing were also sputter-coated with gold and examined in SEM.

One- and two-way analyses of variance were performed to detect significant effects of the variables. Tukey's multiple comparison tests were used to compare the data at p of 0.05.

Results

Figure 1 plots the physical properties of CPC: (A) Setting time, (B) flexural strength, (C) elastic modulus, and (D) work-of-fracture (mean ± standard deviation [sd]; $n=5$). Adding RGD did not change the setting time ($p>0.1$). Strength was (12.1 ± 1.4) MPa for CPC-chitosan-RGD, higher than the (9.9 ± 0.8) MPa for CPC-chitosan control ($p<0.05$). Elastic moduli of the materials were similar ($p>0.05$). Work-of-fracture (toughness) was (103 ± 7) J/m^2 for CPC-chitosan-RGD, higher than (82 ± 6) J/m^2 for control ($p<0.05$). Representative SEM images of the fractured surfaces of CPC-chitosan control are shown in (E) and (F), at a low and high magnification, respectively. As shown in (E), CPC had intrinsic porosity (indicated by P) due to the powder–liquid formulation. The formation of nano- and microcrystals is visible in (F), with arrows indicating small crystalline precipitates. CPC-chitosan-RGD had similar features as shown in (G) and (H), with P indicating porosity, and the arrows indicating fine crystalline precipitates in CPC.

By culturing on MEF feeder in the presence of β-FGF, hESCs were capable of long-term self-renewal, while retaining their pluripotency. The morphology of hESC colonies was shown in Figure 2A. When removed from the MEF feeder and placed in suspension culture, the dissociated hESC clumps formed EBs, which exhibited round shapes (Fig. 2B). EBs differentiated into cells with different morphologies in primary culture. The homogeneity of cell morphology increased with higher passage numbers. In early passages, small groups of cells with a fibroblast-like morphology were observed and became more uniform in size and shape at passages 4 and beyond (Fig. 2C). These hESC-derived cells had a similar morphology to fibroblast and mesenchymal-like cells.

Flow cytometry analysis demonstrated that MSC surface markers were consistently and highly expressed in the hESCd-MSCs (Fig. 3). The MSC surface markers CD29, CD44, CD73, and CD166 were expressed to levels greater than 99.4% in hESCd-MSCs. On the other hand, the expression of hematopoietic markers, CD31, CD34, and CD45 were less than 1.5% in hESCd-MSCs, while the hESC pluripotency markers, TRA-1-81 and Oct3/4, were absent. Furthermore, human leukocyte antigen (HLA) HLA-ABC, present on the surface of all nucleated cells and platelets, was expressed. HLA-DR, usually present only on professional antigen-presenting cells, was absent.

Live/dead results of hESCd-MSCs seeded on CPC-chitosan control and CPC-chitosan-RGD are shown in Figure 4. Live cells (stained green) appeared to have adhered and attained a normal, polygonal morphology and were numerous on both materials. Dead cells were stained red and were relatively few (not shown). Visual examination revealed that the density of live cells adherent to CPC-chitosan-RGD was noticeably more than that on CPC-chitosan control. Over time, live cells increased in numbers due to cell proliferation. The percentage of live cells and live cell density are plotted in (E) and (F) (mean ± sd; $n=5$). Percentage of live cells on CPC-chitosan-RGD was higher compared with control ($p<0.05$). Cell density on CPC-chitosan-RGD was also higher compared with control ($p<0.05$). Due to cell proliferation, increasing the culture time from 1 to 14 days greatly increased the cell density ($p<0.05$). Cell density at 14 days was 6.4-fold of that at 1 day for both CPC-chitosan-RGD and CPC-chitosan control.

Figure 5 shows typical SEM micrographs of hESCd-MSCs on: (A) CPC-chitosan control, (B, C) CPC-chitosan-RGD at 4 days. In (A), cells (designated as C) had healthy polygonal shapes and were anchored to CPC. Compared to CPC-chitosan control, there were noticeably more cells on CPC-

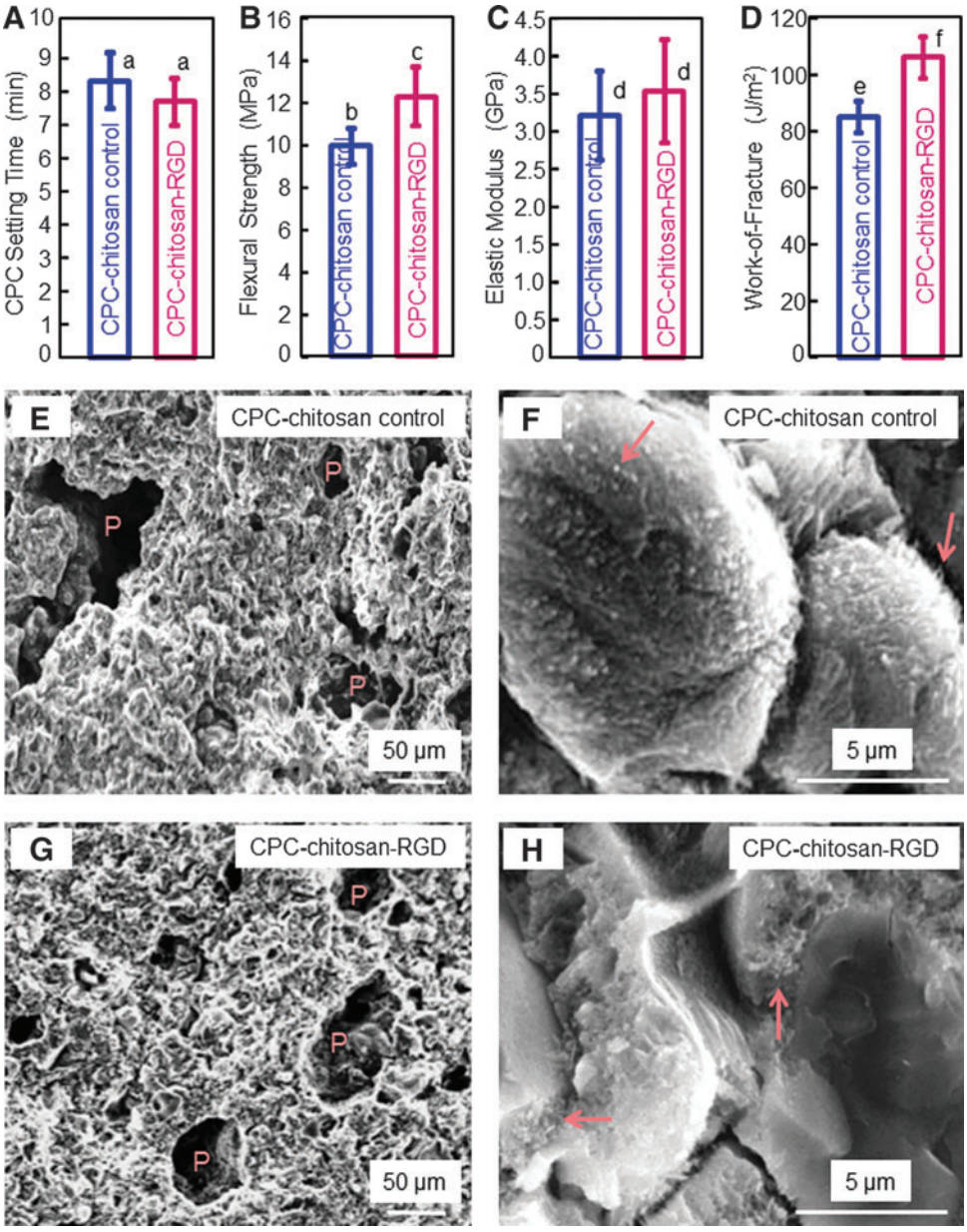

FIG. 1. Effect of RGD immobilization in calcium phosphate cement (CPC) on physical properties: **(A)** Setting time, **(B)** flexural strength, **(C)** elastic modulus, **(D)** work-of-fracture (toughness), **(E, F)** scanning electron micrographs of fracture surfaces of CPC-chitosan-RGD scaffold at a low and high magnification, respectively. Each value is mean ± standard deviation (sd); $n = 5$. In each plot, bars with dissimilar letters are significantly different ($p < 0.05$). RGD immobilization in CPC significantly increased the strength and toughness of CPC. The microstructures of CPC on fractured cross sections are shown in scanning electron microscope (SEM) images in **(E, F)** for CPC-chitosan control, and **(G, H)** for CPC-chitosan-RGD, at low and high magnifications, respectively. "P" indicates the intrinsic pores in CPC resulting from the powder–liquid mixing of the cement. Arrows indicate the fine crystallites that make up the CPC matrix. Color images available online at www.liebertpub.com/tea

chitosan-RGD (example in B). The cells had developed long cytoplasmic extensions E, which are visible in both (A) and (B). A higher magnification of the cell with extension attaching to the scaffold is shown for CPC-chitosan-RGD in (C). These extensions are regions of the cell plasma membrane that contain a meshwork or bundles of actin containing microfilaments, which permit the movement of the migrating cells along a substratum.[47] The healthy spreading morphology and cytoplasmic extensions are indicative of good viability and attachment of hESCd-MSCs to CPC.

ALP, OC, collagen I, and Runx2 gene expressions measured by RT-PCR are plotted in Figure 6. hESCd-MSCs on CPC-chitosan control and CPC-chitosan-RGD showed osteogenic differentiation, with ALP peaking at 7 days. OC, Coll I, and Runx2 peaked at 14 days. CPC-RGD had higher ALP and Runx2 peaks than those for CPC-chitosan control, but the values were not significantly different ($p > 0.1$). hESCd-MSCs on CPC-chitosan-RGD had significantly higher OC and Coll I peaks than those on CPC-chitosan control ($p < 0.05$).

Typical mineral staining photos of the hESCd-MSCs on CPC-chitosan control and CPC-chitosan-RGD are shown in Figure 7. The cells synthesized little mineral (dark red staining) at 7 days. Mineral synthesis increased from 7 to 21 days for both scaffolds. The mineral staining was noticeably thicker and denser for CPC-chitosan-RGD than for CPC-chitosan control, in all five disks per material per time point. At 21 days, a layer of matrix mineralization synthesized by the cells was observed to cover the entire surface of CPC-chitosan-RGD disks. Data from the osteogenesis assay are plotted in (G). At 14 or 21 days, hESCd-MSCs made about twice as much mineral on CPC-chitosan-RGD compared with CPC-chitosan control. These results demonstrate that hESCd-MSCs seeded on CPC were successfully

differentiated into the osteogenic lineage, and hESCd-MSCs mineralization was greatly enhanced by incorporating RGD into CPC.

Discussion

hESCs are highly promising for tissue engineering due to their ability to provide unlimited stem cells with potent differentiation potential. However, only a few studies have investigated hESCs for bone tissue engineering.[13,23–25] There has been no report on hESC-derived MSC seeding on CPC. In a recent study, hESC-derived MSCs were encapsulated in alginate hydrogel microbeads and the microbeads were then incorporated into CPC; there was no direct cell attachment to the CPC surface.[48] In the present study, hESCd-MSCs were seeded on CPC-chitosan and CPC-chitosan-RGD surfaces for osteogenic differentiation and bone mineral synthesis for the first time. Deriving MSCs from hESCs before specific differentiation has the advantage of producing a source of multipotent progenitor cells, which then can be expanded and differentiated into specific lineages, such as bone, cartilage, or fat.[49,50] This strategy can potentially yield a great amount of progenitor cells to regenerate skeletal defects. Therefore, the present study differentiated hESCs into hMSCs before osteogenic differentiation. After an expansion period of four passages, hESCd-MSCs exhibited a uniform fibroblast-like morphology and expressed high levels of hMSCs surface markers consistent with previous studies on MSCs.[23,51,52] The hESCd-MSCs lacked expression of hematopoietic lineage markers,[51,52] hESC pluripotency markers TRA-1-81 and Oct3/4,[53,54] and marker of professional antigen-presenting cells (HLA-DR).[52,55] These findings confirmed that the hESCd-MSCs and hMSCs are highly comparable.

Recent studies showed that hESCs could be guided to differentiate down the osteogenic lineage with a high potential for bone regeneration.[13] Osteogenic differentiation of hESCs were achieved by introducing hESCs or hESCd-MSCs in the osteogenic medium[56,57] or cocultured with other cells.[58,59] Several types of scaffolds, such as collagen,[23] hydrogels,[25] polymer and composite,[13,24] were seeded with hESC-derived cells. However, few studies investigated the hESC seeding on biomaterials with high strength for load-bearing bone tissue engineering.[60] In the present study, hESCs were differentiated into hMSCs and seeded on a mechanically strong CPC with RGD immobilization. CPC is a promising carrier for injectable delivery of stem cells in moderate load-bearing areas for bone regeneration. One of the advantages of CPC is its injectability for minimally invasive surgeries. CPC can be injected or molded to the desired shape, set to form a scaffold *in situ*, and then be resorbed and replaced by new bone.[61] However, the brittleness of CPC limited its application. Chitosan and its derivatives are natural biopolymers found in arthropod exoskeletons. They are biocompatible, biodegradable, and osteoconductive. The incorporation of chitosan into CPC strengthened the CPC.[39,40] In the present study, the G4RGDSP sequence was incorporated into chitosan by formation of imide bonds between amino groups on the chitosan and carboxyl groups on the peptide. EDC and Sulfo-NHS were involved in this reaction, forming intermediate reactants that led to the formation of imide bonds.[62,63] RGD-

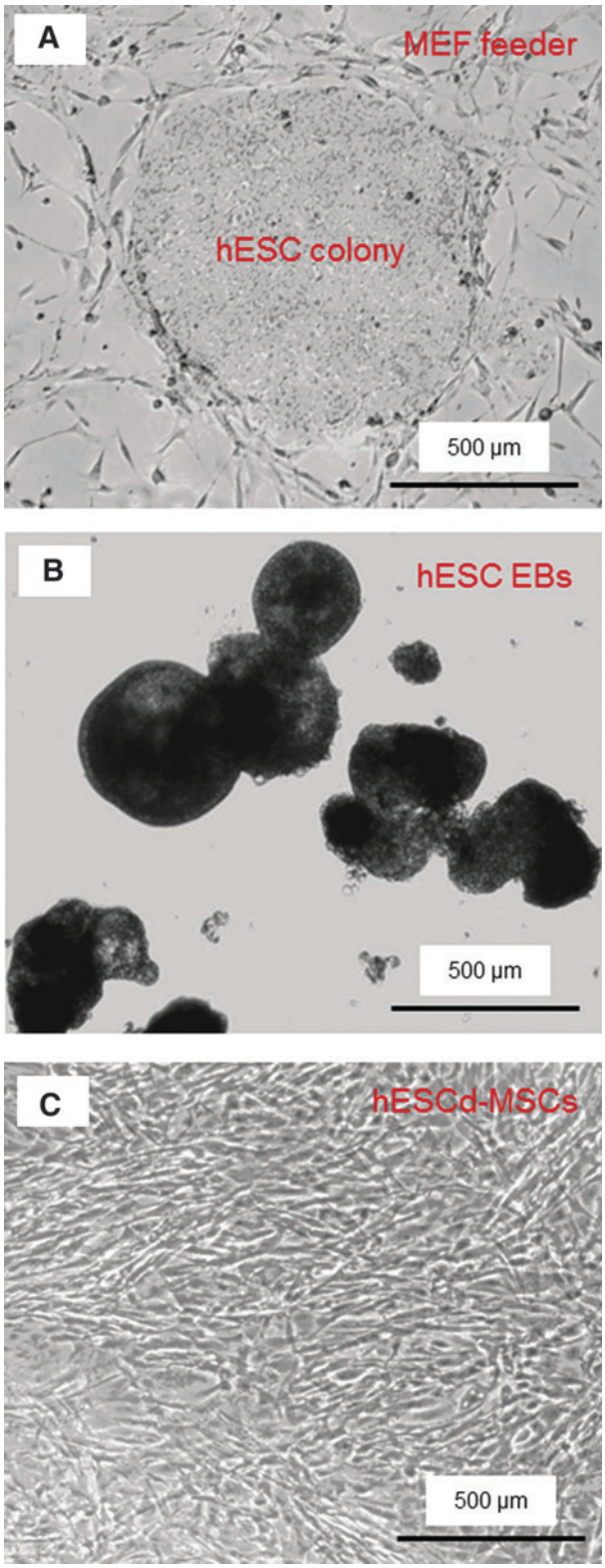

FIG. 2. Phase-contrast photos of human embryonic stem cells (hESC) culture. **(A)** hESC colony cultured on mouse embryonic fibroblast (MEF) feeder layer (example shown at 4 days). **(B)** Embryoid bodies (EBs) formed after 4 days of suspension culture. **(C)** MSCs that migrated out of the EBs were harvested and passaged. The example in **(C)** shows hESC-derived MSCs after passage 4. MSCs, mesenchymal stem cells. Color images available online at www.liebertpub.com/tea

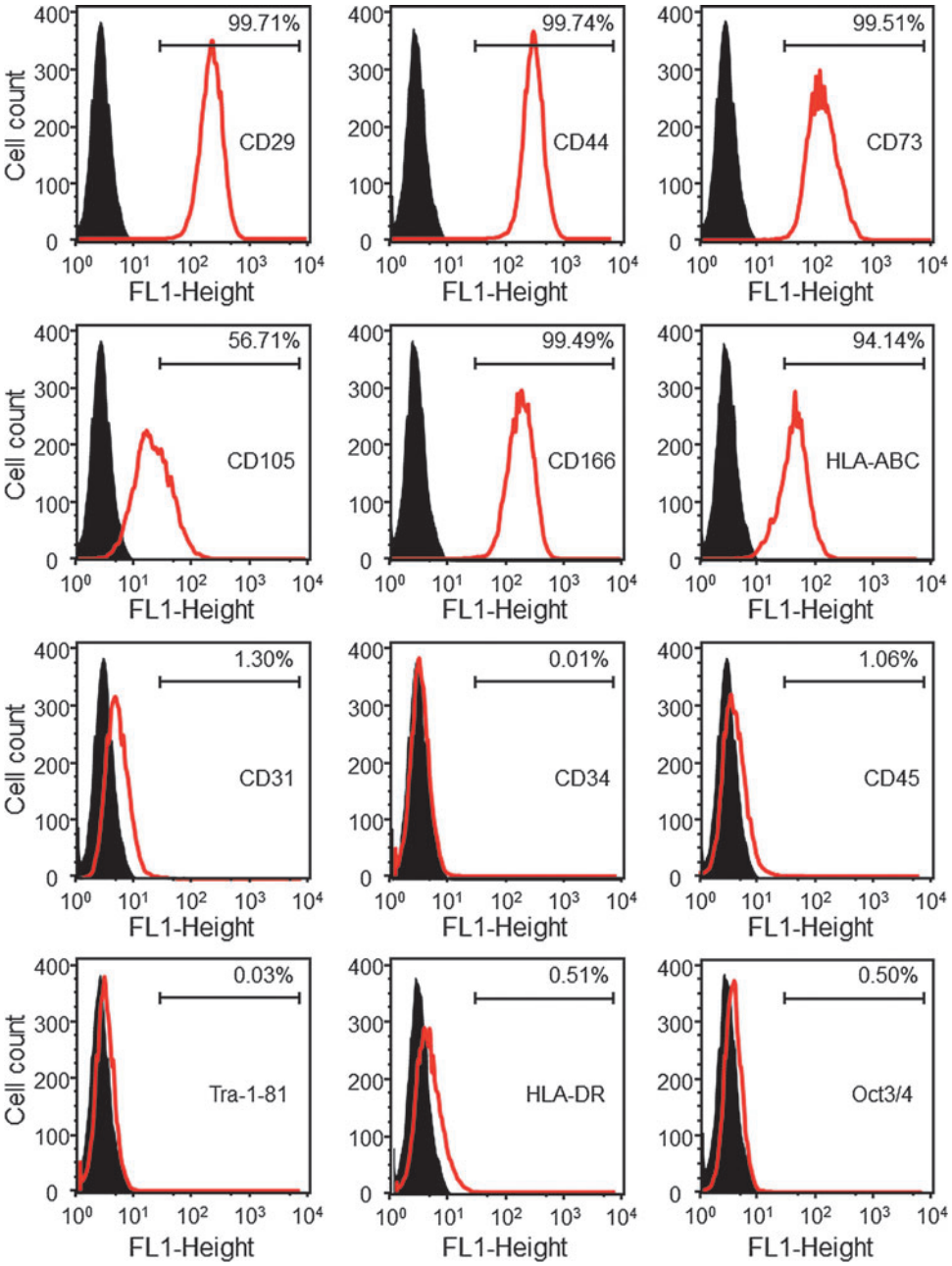

FIG. 3. Flow cytometry analysis of surface markers of hESC-derived MSCs (passage 4 MSCs). The names of the antigens are listed inside each plot. The black histogram represents isotype controls and the red histogram represents the conjugated antibody of each antigen. The number in each plot represents the percentage of positive cells. hESC-derived mesenchymal stem cells (hESCd-MSCs) expressed typical surface antigen profile of MSCs. For example, MSC surface markers CD29, CD44, CD73, and CD166 were expressed to levels greater than 99.4%, while expressions of hematopoietic markers (CD31, CD34, and CD45) were less than 1.5%. Color images available online at www.liebertpub.com/tea

modified chitosan increased the strength and toughness of CPC by approximately 25%. RGD was covalently bonded with chitosan in the present study. It was noticed that the RGD-chitosan liquid was significantly more viscous compared with the chitosan control liquid without RGD, likely because the RGD covalent bonding increased the complexity of the chitosan molecules. It is possible that the more viscous and stickier RGD-functionalized chitosan served as a better gelling agent to bind the CPC components together, yielding a stronger scaffold with higher strength and toughness. A previous study found that pastes with a higher viscosity, once set or polymerized, possessed higher mechanical properties.[64] Another study found that the cement viscosity affected the bonded interface,[65] which suggests that the more viscous and stickier RGD-functionalized chitosan likely had better bonding with the ceramic particles in CPC. While these factors likely contributed to a higher strength and toughness (Fig. 1), there was no significant increase in elastic modulus. Ceramics are typically much stiffer than polymers. The CPC phase in the CPC-chitosan composite scaffold likely dominated the elastic modulus (or stiffness) of the scaffold. In both the CPC-chitosan composite and the CPC-chitosan-RGD composite, chitosan and chitosan-RGD are soft phases, while the CPC phase is the same in both types of scaffolds. This likely contributed to both scaffolds having similar elastic moduli. Further studies are needed to understand the chitosan-RGD contribution to the mechanical properties of the CPC scaffold. Mechanical properties of scaffolds are useful in orthopedic, dental, and craniofacial applications. The good mechanical properties of CPC-RGD could enable its use in mandibular and maxillary regenerations, periodontal bone repair, as well as other moderate load-bearing orthopedic applications.

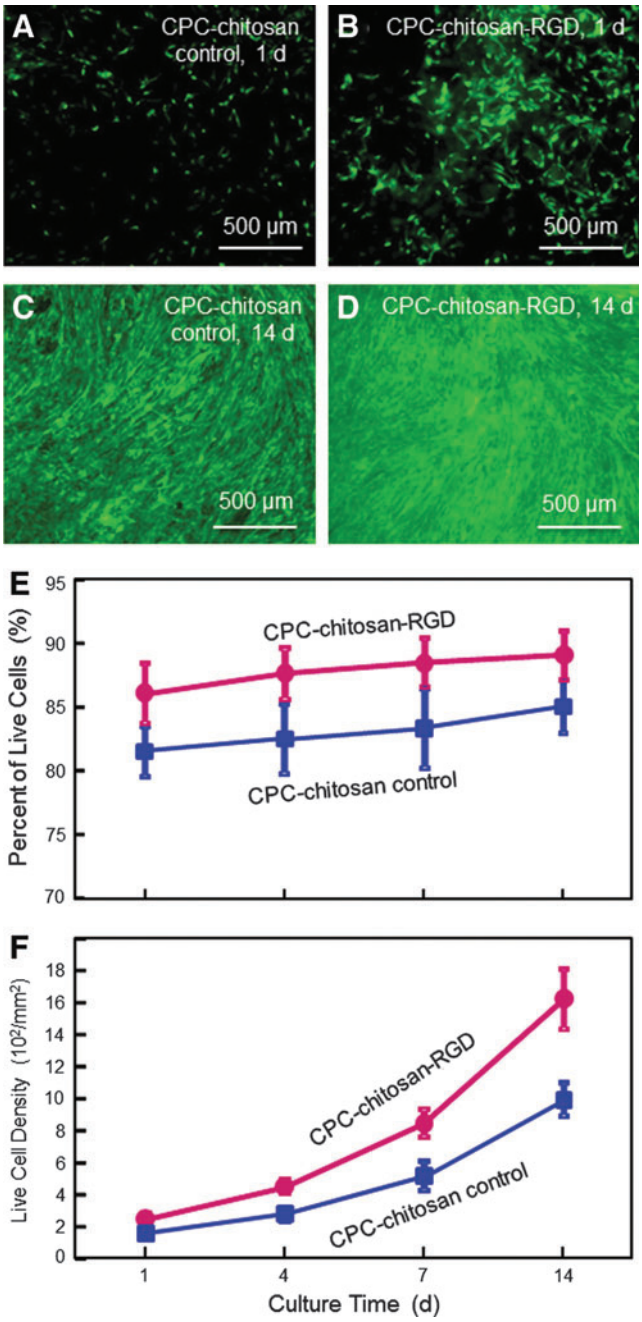

FIG. 4. Viability of hESCd-MSCs cultured on CPC-chitosan control and CPC-chitosan-RGD. **(A–D)** Representative photos of hESCd-MSCs. Live cells were stained green and were numerous on both scaffolds. Dead cells (stained red, not shown here) were relatively few. **(E)** The percentage of live cells. **(F)** Live cell density (number of live cells per mm^2), which increased with time due to cell proliferation. Each value is mean ± sd; $n = 5$. Incorporation of RGD into CPC significantly improved the hESCd-MSCs attachment. Color images available online at www.liebertpub.com/tea

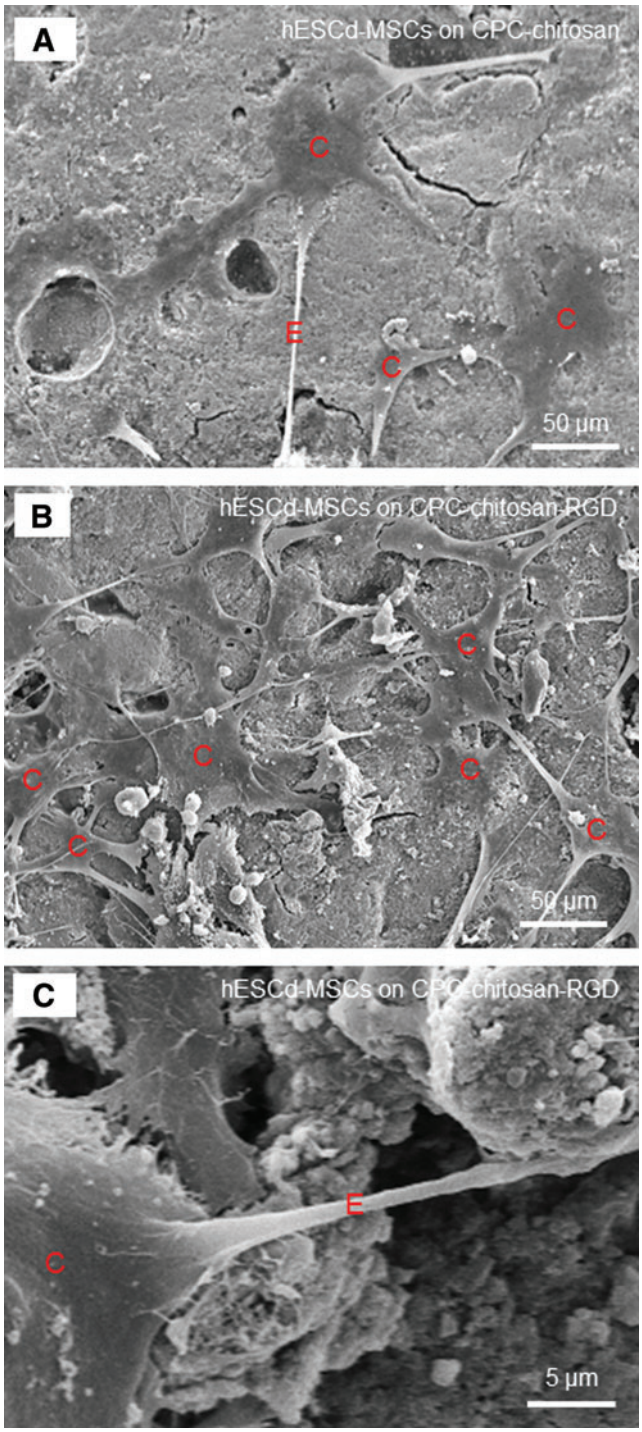

FIG. 5. SEM micrographs of hESCd-MSCs attachment on: **(A)** CPC-chitosan control, and **(B, C)** CPC-chitosan-RGD at 4 days. Cells are designated as C. The cells had developed a healthy spreading and polygonal morphology. There were noticeably more cells attaching to CPC-chitosan-RGD than to CPC-chitosan control. The cells had developed long cytoplasmic extensions E, which is shown in **(C)** at a higher magnification. Color images available online at www.liebertpub.com/tea

Previous studies showed that human stem cell attachment to CPC was relatively poor.[40,41] The tripeptide RGD sequence can promote the attachment of cells because it is recognized by the adhesion receptors on the cell membrane. Thus, the affinity between cells and biomaterials could be improved by the immobilization of RGD, which can mimic the natural extracellular matrix. As the most effective and most frequently used peptide sequence to stimulate cell adhesion, RGD has been applied to many biomaterials, such as glass, polymers, and ceramics, to improve cell adhesion.

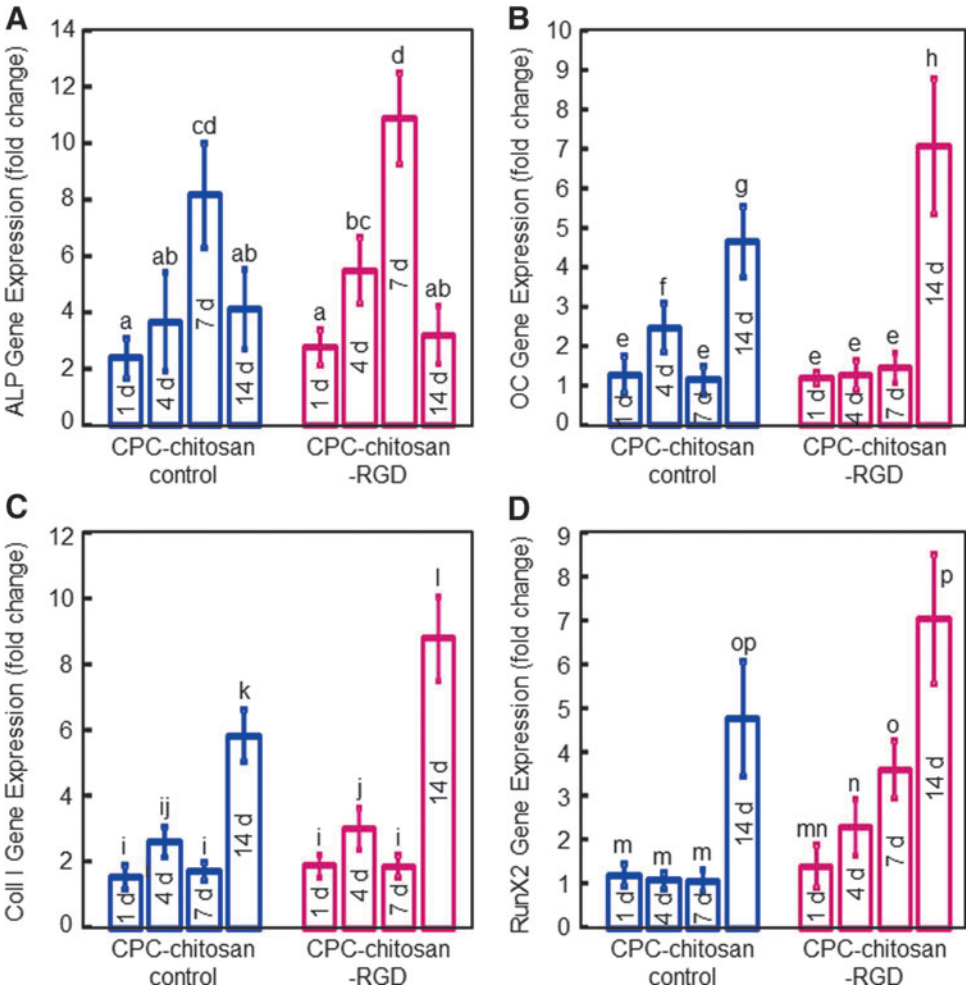

FIG. 6. RT-PCR results for osteogenic differentiation of hESCd-MSCs on CPC-chitosan control and CPC-chitosan-RGD: **(A)** Alkaline phosphatase (ALP), **(B)** Osteocalcin (OC), **(C)** Collagen type I (Coll I), and **(D)** Runx2 gene expressions. Each value is mean ± sd; $n = 5$. hESCd-MSCs attaching to both scaffolds showed osteogenic differentiation. The ALP peaked at 7 days. The OC, Coll I, and Runx2 peak at 14 days. In each plot, values with dissimilar letters are significantly different ($p < 0.05$). Color images available online at www.liebertpub.com/tea

Injectable CPC is a promising matrix for the development of scaffolds with RGD features. However, a literature search revealed no report on RGD incorporation into CPC. In the present study, under the same culture conditions, CPC-chitosan-RGD had 246 cells/mm^2 at 1 day, compared to 153 cells/mm^2 at 1 day for CPC-chitosan control. This showed that the initial attachment of hESCd-MSCs was increased by 1.6 times via immobilization of RGD in the chitosan in CPC. This was consistent with SEM examinations, which showed that there were substantially more hESCd-MSCs adhering to CPC-chitosan-RGD than to CPC-chitosan control. At 14 days, CPC-chitosan-RGD had 1622 cells/mm^2, compared to 994 cells/mm^2 on CPC-chitosan control. Hence, CPC-chitosan-RGD had a cell density that was 1.6 times that on CPC control at 14 days, the same ratio as that at 1 day. Hence, while RGD in CPC promoted the hESCd-MSC attachment at 1 day, it did not increase cell proliferation by 14 days. This may be because the CPC-chitosan-RGD specimen had many more cells, and hence, there was more local contact inhibition than cells on CPC control. Hence, the higher cell density on CPC-chitosan-RGD may have limited further cell proliferation. Further study using the macroporous three-dimensional CPC scaffold with more space for cell proliferation is needed to investigate the effect of RGD-modification on cell proliferation in CPC. The present study showed for the first time that RGD modification of CPC (1) increased the strength and toughness of CPC, (2) increased the hESCd-MSC attachment to CPC, (3) achieved a much higher cell density at 14 days on CPC-chitosan-RGD compared with CPC-chitosan control.

hESCd-MSCs on CPC-chitosan-RGD differentiated into the osteogenic lineage, with high expressions of osteogenic markers and mineral synthesis. Gene expressions of ALP, OC, Coll I, and Runx2 play key roles in the osteogenic differentiation of MSCs.[66] As an enzyme expressed in the early stage of MSC osteogenesis, ALP is a well-defined marker for differentiation. As the cascade of events for the differentiation continues, other markers, such as OC, Coll I, and Runx2, also become upregulated.[66] This is consistent with the results of the present study on hESCd-MSCs, which showed that while ALP peaked at 7 days, OC, Coll I, and Runx2 peaked at 14 days. In addition, the present study showed that cells on CPC-chitosan-RGD had moderately higher osteogenic gene expressions than those on CPC-chitosan control. The RT-PCR results represent the average gene expression level of cells in each scaffold; hence, a larger RT-PCR value represents a higher gene expression per cell and not because there were more cells in the scaffold. The observation that RGD in CPC promoted osteogenic gene expressions is in agreement with previous studies using different substrates and different types of cells.[12,67,68] The amount of minerals synthesized by hESCd-MSCs was much more on CPC-

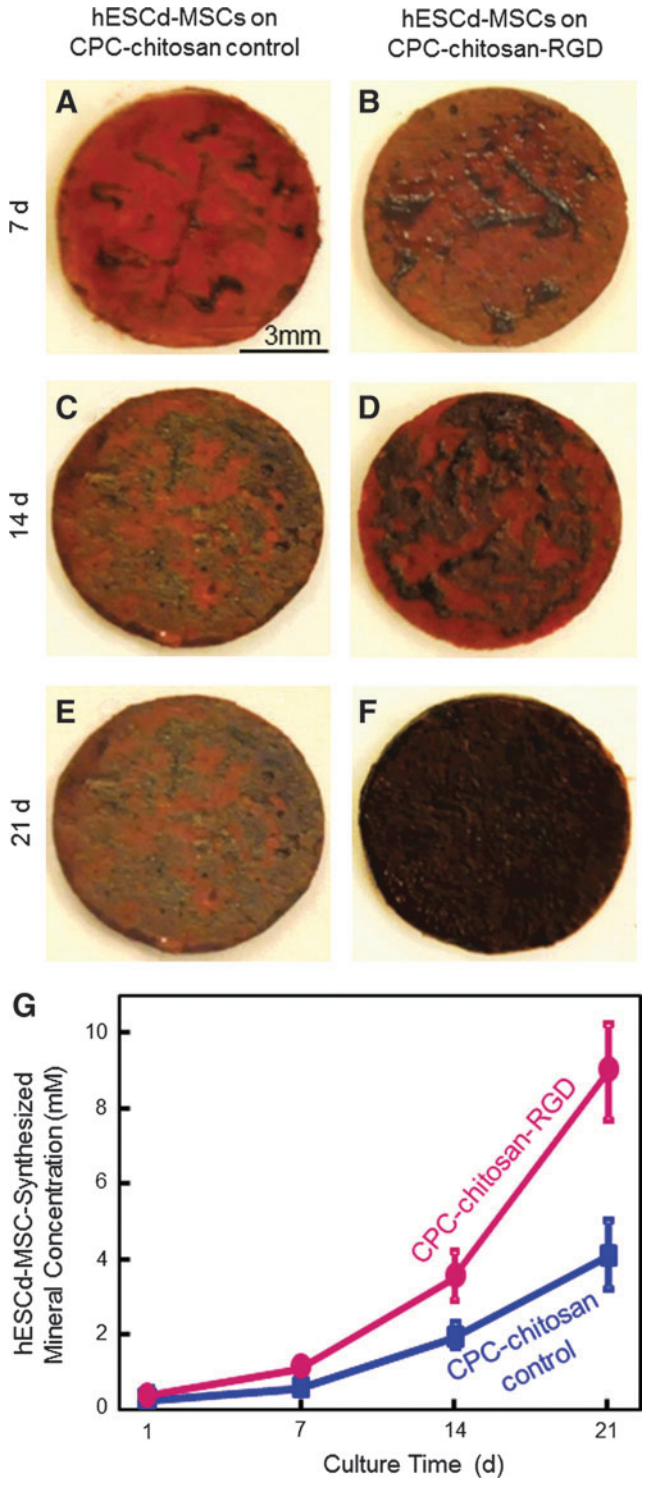

FIG. 7. Mineral synthesis by hESCd-MSCs on CPC-chitosan-RGD and CPC-chitosan control: **(A, B)** 7 days, **(C, D)** 14 days, and **(E, F)** 21 days. **(G)** Results from the osteogenesis assay (mean ± sd; $n = 5$). Mineral synthesis by the cells increased with time for both scaffolds. Mineral synthesis by cells on CPC-chitosan-RGD was 2-fold of that on CPC-chitosan control at 21 days. Color images available online at www.liebertpub.com/tea

chitosan-RGD than on CPC-chitosan control. This is likely because cells on CPC-chitosan-RGD had better attachment, and there were more cells on CPC-chitosan-RGD than CPC-chitosan control, which contributed to much more mineral synthesis. It should be noted that the mineral synthesis by cells on CPC-chitosan-RGD were greatly increased, while the RT-PCR results for CPC-chitosan-RGD were only slightly increased, compared to CPC-chitosan control. This is because two factors contributed to the amount of mineral synthesis: (1) More cells on CPC-chitosan-RGD due to better cell attachment; and (2) enhanced osteogenic differentiation per cell on CPC-chitosan-RGD. In contrast, only factor 2 contributed to the RT-PCR results, because the RT-PCR results were related to gene expression per cell. Therefore, it can be concluded that hESCd-MSCs synthesized much more minerals on CPC-chitosan-RGD than on CPC-chitosan control, resulting from slightly enhanced osteogenic differentiation per cell, but many more cells due to better cell attachment on CPC-chitosan-RGD. Hence, this study demonstrated that: (1) MSCs could be successfully derived from hESCs, which were compatible with CPC and yielded excellent proliferation and differentiation; (2) CPC could be a promising carrier to deliver hESCd-MSCs for bone tissue engineering; (3) RGD-immobilized chitosan incorporation into CPC greatly increased hESCd-MSC attachment and live cell density on the CPC-chitosan-RGD scaffold. Further study is needed to evaluate the hESCd-MSCs delivered via CPC-chitosan-RGD for bone regeneration in an animal model.

Conclusions

This study immobilized RGD in chitosan for incorporation into a self-setting CPC, and investigated hESCd-MSCs proliferation and osteogenic differentiation on CPC-chitosan-RGD for the first time. MSCs were obtained by culturing hESC colonies and EBs. The hESCd-MSCs were shown to be compatible with CPC, resulting in good cell viability, fast proliferation, highly elevated osteogenic marker expressions, and bone mineral synthesis. RGD incorporation into CPC significantly increased the strength and toughness of CPC without adversely affecting the cement setting time. hESCd-MSC attachment on CPC-chitosan-RGD was improved by 60%, compared to that on CPC-chitosan control. hESCd-MSCs proliferated well on CPC-chitosan-RGD and increased live cell density by 6.4-fold from 1 to 14 days. Osteogenic marker expressions were enhanced with RGD in CPC. Mineral synthesis by hESCd-MSCs on CPC-chitosan-RGD was twice that on CPC-chitosan control at 21 days. Therefore, the novel CPC-chitosan-RGD scaffold increased hESCd-MSC attachment, live cell density, osteogenic expressions, and mineralization. These results support the promise of hESCd-MSCs for bone tissue engineering. The strong CPC-chitosan-RGD scaffold seeded with hESCd-MSCs with excellent proliferation and differentiation may be useful for orthopedic and craniofacial applications.

Acknowledgments

We are indebted to Dr. Ferenc Livak for help with flow cytometry that was performed at the University of Maryland Greenbaum Cancer Center Shared Flow Cytometry Facility. We thank Dr. Larry C. Chow and Dr. Carl G. Simon for discussions. We also thank Prof. Xuedong Zhou and Prof.

Qianming Chen for help. This study was supported by NIH R01 grant DE14190 and R21 DE22625 (HX), National Science foundation of China NSFC-30970728 (CB), Maryland Stem Cell Fund (HX), University of Maryland School of Dentistry, and West China School of Stomatology.

Disclosure Statement

No competing financial interests exist.

References

1. Cutter, C.S., and Mehrara, B.J. Bone grafts and substitutes. J Long Term Eff Med Implants **16,** 249, 2006.
2. Johnson, P.C., Mikos, A.G., Fisher, J.P., and Jansen, J.A. Strategic directions in tissue engineering. Tissue Eng **13,** 2827, 2007.
3. Laurencin, C.T., Ambrosio, A.M., Borden, M.D., and Cooper, J.A., Jr. Tissue engineering: orthopedic applications. Annu Rev Biomed Eng **1,** 19, 1999.
4. Mistry, A.S., and Mikos, A.G. Tissue engineering strategies for bone regeneration. Adv Biochem Eng Biotechnol **94,** 1, 2005.
5. Tuan, R.S., Boland, G., and Tuli, R. Adult mesenchymal stem cells and cell-based tissue engineering. Arthritis Res Ther **5,** 32, 2003.
6. Castano-Izquierdo, H., Alvarez-Barreto, J., van den Dolder, J., Jansen, J.A., Mikos, A.G., and Sikavitsas, V.I. Pre-culture period of mesenchymal stem cells in osteogenic media influences their *in vivo* bone forming potential. J Biomed Mater Res A **82,** 129, 2007.
7. Johnson, P.C., and Mikos, A.G. Stem cells: state of the art. In: Johnson, P.C., and Mikos, A.G. eds. Advances in Tissue Engineering, Volume 2: Stem Cells. New Rochelle, NY: Mary Ann Liebert, Inc., 2010, p. 3.
8. Guo, X., Park, H., Young, S., Kretlow, J.D., van den Beucken, J.J., Baggett, L.S., Tabata, Y., Kasper, F.K., Mikos, A.G., and Jansen, J.A. Repair of osteochondral defects with biodegradable hydrogel composites encapsulating marrow mesenchymal stem cells in a rabbit model. Acta Biomater **6,** 39, 2010.
9. Mao, J.J., Giannobile, W.V., Helms, J.A., Hollister, S.J., Krebsbach, P.H., Longaker, M.T., and Shi, S. Craniofacial tissue engineering by stem cells. J Dent Res **85,** 966, 2006.
10. Varghese, S., Hwang, N.S., Ferran, A., Hillel, A., Theprungsirikul, P., Canver, A.C., Zhang, Z., Gearhart, J., and Elisseeff, J. Engineering musculoskeletal tissues with human embryonic germ cell derivatives. Stem Cells **28,** 765, 2010.
11. Benoit, D.S., Nuttelman, C.R., Collins, S.D., and Anseth, K.S. Synthesis and characterization of a fluvastatin-releasing hydrogel delivery system to modulate hMSC differentiation and function for bone regeneration. Biomaterials **27,** 6102, 2006.
12. Hsiong, S.X., Boontheekul, T., Huebsch, N., and Mooney, D.J. Cyclic arginine-glycine-aspartate peptides enhance three-dimensional stem cell osteogenic differentiation. Tissue Eng Part A **15,** 263, 2009.
13. Kim, S., Kim, S.S., Lee, S.H., Eun, A.S., Gwak, S.J., Song, J.H., Kim, B.S., and Chung, H.M. *In vivo* bone formation from human embryonic stem cell-derived osteogenic cells in poly(D,L-lactic-co-glycolic acid)/hydroxyapatite composite scaffolds. Biomaterials **29,** 1043, 2008.
14. Baksh, D., Yao, R., and Tuan, R.S. Comparison of proliferative and multilineage differentiation potential of human mesenchymal stem cells derived from umbilical cord and bone marrow. Stem Cells **25,** 1384, 2007.
15. Alhadlaq, A., and Mao, J.J. Mesenchymal stem cells: isolation and therapeutics. Stem Cells Dev **13,** 436, 2004.
16. Rahaman, M.N., and Mao, J.J. Stem cell-based composite tissue constructs for regenerative medicine. Biotechnol Bioeng **91,** 261, 2005.
17. Mueller, S.M., and Glowacki, J. Age-related decline in the osteogenic potential of human bone marrow cells cultured in three-dimensional collagen sponges. J Cell Biochem **82,** 583, 2001.
18. Mendes, S.C., Tibbe, J.M., Veenhof, M., Bakker, K., Both, S., Platenburg, P.P., Oner, F.C., de Bruijn, J.D., and van Blitterswijk, C.A. Bone tissue-engineered implants using human bone marrow stromal cells: effect of culture conditions and donor age. Tissue Eng **8,** 911, 2002.
19. Stenderup, K., Justesen, J., Clausen, C., and Kassem, M. Aging is associated with decreased maximal life span and accelerated senescence of bone marrow stromal cells. Bone **33,** 919, 2003.
20. Rodriguez, J.P., Montecinos, L., Rios, S., Reyes, P., and Martinez, J. Mesenchymal stem cells from osteoporotic patients produce a type I collagen-deficient extracellular matrix favoring adipogenic differentiation. J Cell Biochem **79,** 557, 2000.
21. Suzuki, Y., Kim, K.J., Kotake, S., and Itoh, T. Stromal cell activity in bone marrow from the tibia and iliac crest of patients with rheumatoid arthritis. J Bone Miner Metab **19,** 56, 2001.
22. Quarto, R., Thomas, D., and Liang, C.T. Bone progenitor cell deficits and the age-associated decline in bone repair capacity. Calcif Tissue Int **56,** 123, 1995.
23. Arpornmaeklong, P., Brown, S.E., Wang, Z., and Krebsbach, P.H. Phenotypic characterization, osteoblastic differentiation, and bone regeneration capacity of human embryonic stem cell-derived mesenchymal stem cells. Stem Cells Dev **18,** 955, 2009.
24. Lee, S.J., Lim, G.J., Lee, J.W., Atala, A., and Yoo, J.J. *In vitro* evaluation of a poly(lactide-co-glycolide)-collagen composite scaffold for bone regeneration. Biomaterials **27,** 3466, 2006.
25. Horak, D., Matulka, K., Hlidkova, H., Lapcikova, M., Benes, M.J., Jaros, J., Hampl, A., and Dvorak, P. Pentapeptide-modified poly(N,N-diethylacrylamide) hydrogel scaffolds for tissue engineering. J Biomed Mater Res B Appl Biomater **98,** 54, 2011.
26. Chaikof, E.L., Matthew, H., Kohn, J., Mikos, A.G., Prestwich, G.D., and Yip, C.M. Biomaterials and scaffolds in reparative medicine. Ann N Y Acad Sci **961,** 96, 2002.
27. Foppiano, S., Marshall, S.J., Marshall, G.W., Saiz, E., and Tomsia, A.P. The influence of novel bioactive glasses on *in vitro* osteoblast behavior. J Biomed Mater Res A **71,** 242, 2004.
28. Deville, S., Saiz, E., Nalla, R.K., and Tomsia, A.P. Freezing as a path to build complex composites. Science **311,** 515, 2006.
29. Leach, J.K., Kaigler, D., Wang, Z., Krebsbach, P.H., and Mooney, D.J. Coating of VEGF-releasing scaffolds with bioactive glass for angiogenesis and bone regeneration. Biomaterials **27,** 3249, 2006.
30. Ginebra, M.P., Driessens, F.C., and Planell, J.A. Effect of the particle size on the micro and nanostructural features of a calcium phosphate cement: a kinetic analysis. Biomaterials **25,** 3453, 2004.
31. Ginebra, M.P., Traykova, T., and Planell, J.A. Calcium phosphate cements as bone drug delivery systems: a review. J Control Release **113,** 102, 2006.

32. Jansen, J.A., Vehof, J.W., Ruhe, P.Q., Kroeze-Deutman, H., Kuboki, Y., Takita, H., Hedberg, E.L., and Mikos, A.G. Growth factor-loaded scaffolds for bone engineering. J Control Release **101,** 127, 2005.
33. Salinas, C.N., and Anseth, K.S. The influence of the RGD peptide motif and its contextual presentation in PEG gels on human mesenchymal stem cell viability. J Tissue Eng Regen Med **2,** 296, 2008.
34. Bohner, M. Design of ceramic-based cements and putties for bone graft substitution. Eur Cell Mater **20,** 1, 2010.
35. Brown, W.E., and Chow, L.C. A new calcium phosphate water setting cement. In: Brown, P.W., ed. Cements Research Progress. Westerville, OH: American Ceramic Society, 1986, p. 352.
36. Bohner, M., and Baroud, G. Injectability of calcium phosphate pastes. Biomaterials **26,** 1553, 2005.
37. Link, D.P., van den Dolder, J., van den Beucken, J.J., Wolke, J.G., Mikos, A.G., and Jansen, J.A. Bone response and mechanical strength of rabbit femoral defects filled with injectable CaP cements containing TGF-beta 1 loaded gelatin microparticles. Biomaterials **29,** 675, 2008.
38. Friedman, C.D., Costantino, P.D., Takagi, S., and Chow, L.C. BoneSource hydroxyapatite cement: a novel biomaterial for craniofacial skeletal tissue engineering and reconstruction. J Biomed Mater Res **43,** 428, 1998.
39. Xu, H.H.K., and Simon, C.G., Jr. Fast setting calcium phosphate-chitosan scaffold: mechanical properties and biocompatibility. Biomaterials **26,** 1337, 2005.
40. Weir, M.D., and Xu, H.H.K. Culture human mesenchymal stem cells with calcium phosphate cement scaffolds for bone repair. J Biomed Mater Res B Appl Biomater **93,** 93, 2010.
41. Link, D.P., van den Dolder, J., Wolke, J.G., and Jansen, J.A. The cytocompatibility and early osteogenic characteristics of an injectable calcium phosphate cement. Tissue Eng **13,** 493, 2007.
42. Xu, H.H.K., Takagi, S., Quinn, J.B., and Chow, L.C. Fast-setting calcium phosphate scaffolds with tailored macropore formation rates for bone regeneration. J Biomed Mater Res A **68,** 725, 2004.
43. Park, K.M., Joung, Y.K., Park, K.D., Lee, S.Y., and Lee, M.C. RGD-conjugated chitosan-pluronic hydrogels as a cell supported scaffold for articular cartilage regeneration. Macromol Res **16,** 517, 2008.
44. Thomson, J.A., Itskovitz-Eldor, J., Shapiro, S.S., Waknitz, M.A., Swiergiel, J.J., Marshall, V.S., and Jones, J.M. Embryonic stem cell lines derived from human blastocysts. Science **282,** 1145, 1998.
45. Livak, K.J., and Schmittgen, T.D. Analysis of relative gene expression data using real-time quantitative PCR and the 2(-Delta Delta C(T)) Method. Methods **25,** 402, 2001.
46. Wang, Y.H., Liu, Y., Maye, P., and Rowe, D.W. Examination of mineralized nodule formation in living osteoblastic cultures using fluorescent dyes. Biotechnol Prog **22,** 1697, 2006.
47. Lodish, H., Berk, A., Zipursky, S.L., Matsudaira, P., Baltimore, D., and Darnell, J. Molecular Cell Biology, 3rd edition. New York: W. H. Freeman & Company, 2000, Chapter 18.
48. Tang, M., Chen, W., Weir, M.D., Thein-Han, W., and Xu, H.H.K. Human embryonic stem cell-encapsulation in alginate microbeads in macroporous calcium phosphate cement for bone tissue engineering. Acta Biomater **8,** 3436, 2012.
49. Heng, B.C., Cao, T., Stanton, L.W., Robson, P., and Olsen, B. Strategies for directing the differentiation of stem cells into the osteogenic lineage *in vitro*. J Bone Miner Res **19,** 1379, 2004.
50. Fenno, L.E., Ptaszek, L.M., and Cowan, C.A. Human embryonic stem cells: emerging technologies and practical applications. Curr Opin Genet Dev **18,** 324, 2008.
51. Trivedi, P., and Hematti, P. Simultaneous generation of CD34+ primitive hematopoietic cells and CD73+ mesenchymal stem cells from human embryonic stem cells co-cultured with murine OP9 stromal cells. Exp Hematol **35,** 146, 2007.
52. Trivedi, P., and Hematti, P. Derivation and immunological characterization of mesenchymal stromal cells from human embryonic stem cells. Exp Hematol **36,** 350, 2008.
53. Gruenloh, W., Kambal, A., Sondergaard, C., McGee, J., Nacey, C., Kalomoiris, S., Pepper, K., Olson, S., Fierro, F., and Nolta, J.A. Characterization and *in vivo* testing of mesenchymal stem cells derived from human embryonic stem cells. Tissue Eng Part A **17,** 1517, 2011.
54. Niwa, H., Miyazaki, J., and Smith, A.G. Quantitative expression of Oct-3/4 defines differentiation, dedifferentiation or self-renewal of ES cells. Nat Genet **24,** 372, 2000.
55. Le, B.K., Tammik, C., Rosendahl, K., Zetterberg, E., and Ringden, O. HLA expression and immunologic properties of differentiated and undifferentiated mesenchymal stem cells. Exp Hematol **31,** 890, 2003.
56. Karp, J.M., Ferreira, L.S., Khademhosseini, A., Kwon, A.H., Yeh, J., and Langer, R.S. Cultivation of human embryonic stem cells without the embryoid body step enhances osteogenesis *in vitro*. Stem Cells **24,** 835, 2006.
57. Olivier, E.N., Rybicki, A.C., and Bouhassira, E.E. Differentiation of human embryonic stem cells into bipotent mesenchymal stem cells. Stem Cells **24,** 1914, 2006.
58. Ahn, S.E., Kim, S., Park, K.H., Moon, S.H., Lee, H.J., Kim, G.J., Lee, Y.J., Park, K.H., Cha, K.Y., and Chung, H.M. Primary bone-derived cells induce osteogenic differentiation without exogenous factors in human embryonic stem cells. Biochem Biophys Res Commun **340,** 403, 2006.
59. Inanc, B., Elcin, A.E., and Elcin, Y.M. Effect of osteogenic induction on the *in vitro* differentiation of human embryonic stem cells cocultured with periodontal ligament fibroblasts. Artif Organs **31,** 792, 2007.
60. Kuznetsov, S.A., Cherman, N., and Robey, P.G. *In vivo* bone formation by progeny of human embryonic stem cells. Stem Cells Dev **20,** 269, 2011.
61. Bohner, M., Gbureck, U., and Barralet, J.E. Technological issues for the development of more efficient calcium phosphate bone cements: a critical assessment. Biomaterials **26,** 6423, 2005.
62. Kouvroukoglou, S., Dee, K.C., Bizios, R., McIntire, L.V., and Zygourakis, K. Endothelial cell migration on surfaces modified with immobilized adhesive peptides. Biomaterials **21,** 1725, 2000.
63. Wissink, M.J., Beernink, R., Poot, A.A., Engbers, G.H., Beugeling, T., van Aken, W.G., and Feijen, J. Relation between cell density and the secretion of von Willebrand factor and prostacyclin by human umbilical vein endothelial cells. Biomaterials **22,** 2283, 2001.
64. Goncalves, F., Kawano, Y., Pfeifer, C., Stansbury, J.W., and Braga, R.R. Influence of BisGMA, TEGDMA, and BisEMA contents on viscosity, conversion, and flexural strength of experimental resins and composites. Eur J Oral Sci **117,** 442, 2009.

65. Miller, M.A., Race, A., Gupta, S., Higham, P., Clarke, M.T., and Mann, K.A. The role of cement viscosity on cement-bone apposition and strength: an *in vitro* model with medullary bleeding. J Arthroplasty **22,** 109, 2007.
66. Kim, K., Dean, D., Mikos, A.G., and Fisher, J.P. Effect of initial cell seeding density on early osteogenic signal expression of rat bone marrow stromal cells cultured on cross-linked poly(propylene fumarate) disks. Biomacromolecules **10,** 1810, 2009.
67. Yang, F., Williams, C.G., Wang, D.A., Lee, H., Manson, P.N., and Elisseeff, J. The effect of incorporating RGD adhesive peptide in polyethylene glycol diacrylate hydrogel on osteogenesis of bone marrow stromal cells. Biomaterials **26,** 5991, 2005.
68. Morgan, A.W., Roskov, K.E., Lin-Gibson, S., Kaplan, D.L., Becker, M.L., and Simon, C.G., Jr. Characterization and optimization of RGD-containing silk blends to support osteoblastic differentiation. Biomaterials **29,** 2556, 2008.

Address correspondence to:
Hockin H.K. Xu, PhD
Biomaterials & Tissue Engineering Division
Department of Endodontics
University of Maryland Dental School
Baltimore, MD 21201

E-mail: hxu@umaryland.edu

Chongyun Bao, DDS, PhD
State Key Laboratory of Oral Diseases
West China College of Stomatology
Sichuan University
Chengdu
Sichuan 610041
China

E-mail: cybao9933@yahoo.com.cn

Received: March 16, 2012
Accepted: October 22, 2012
Online Publication Date: January 28, 2013